Aerosol and Air Quality Research, 15: 46–57, 2015

ISSN: 1680-8584 print / 2071-1409 online
doi: 10.4209/aaqr.2014.03.0041

Diagnostic Analysis of the Sulfate Aerosol Pollution in Spring over Pearl River Delta, China

Qi Fan[1], Jing Lan[2], Yiming Liu[1], Xuemei Wang[1*], Pakwai Chan[3], Shaojia Fan[1], Yingying Hong[1], Yexin Liu[4], Yanjun Zeng[4], Guixiong Liang[4], Yerong Feng[5]

[1] *School of Environmental Science and Engineering, Sun Yat-sen University, 135 Xingang West Road, Guangzhou, China*
[2] *Guangzhou Climate and Agrometeorology Center, 6 Fujin Road, Guangzhou, China*
[3] *Hong Kong Observatory, 134A Nathan Road, Kowloon, Hong Kong, China*
[4] *Guangzhou Environmental Monitoring, 95 Jixiang Road, Guangzhou, China*
[5] *Key Laboratory of Regional Numerical Weather Prediction, 6 Fujin Road, Guangzhou, China*

ABSTRACT

The study of sulfate aerosols has important research significance to atmospheric chemistry and climate change. A diagnostic study on generation mechanism of sulfate aerosol over the PRD region was conducted using sulfate tracking method. Three pollution episodes occurred in March 2012, in which the first two episodes were mostly caused by fine particulate matters and their secondary aerosols were mainly inorganic sulfates, resulting in low visibility. In contrast, the third pollution episode was dominated by coarse particles with relatively greater visibility. The results of sulfate tracking showed that in addition to emission sources and contributions of initial and boundary conditions, sulfate-generating reaction processes were closely correlated with relative humidity. The first two episodes occurred under the influence of southerly warm and wet air flow system with relatively high humidity, in which the conditions were favorable for aqueous reaction processes. The primary type of liquid-phase oxidation was with hydrogen peroxide (H_2O_2), followed by catalytic oxidation with Fe and Mn and oxidation with ozone (O_3), while peroxyacetic acid (PAA) and methylhydroperoxide (MHP) had very small contributions. Meanwhile, the third pollution episode happened during a warming period following passage of a cold front and was influenced by northerly wind system. Consequently, humidity was relatively low, and therefore, contribution of liquid-phase oxidation reactions was weaker while contributions by gas-phase oxidation between S(IV) and hydroxyl radical (OH) became more prominent. In addition, the simulated vertical distribution results showed that the mass concentration of sulfate aerosols decreased with increasing height. For near-surface layers, sulfates were mainly contributed by emission sources, boundary and initial conditions, liquid-phase oxidations with H_2O_2 and catalytic conversions with Fe and Mn; while for upper layers, sulfates were contributed by, in the order of significance, liquid-phase oxidations with H_2O_2, catalytic conversions with Fe and Mn, emission sources and gas-phase oxidations.

Keywords: WRF/SMOKE/CMAQ model system; Sulfate tracking; Liquid-phase oxidation; Gas-phase oxidation.

INTRODUCTION

The rapid urbanization and industrialization in China have caused episodes of complex regional atmospheric pollution in various megalopolises, and problems with aerosol pollution have become more prominent in particular. The Ministry of Environmental Protection of China included $PM_{2.5}$ in its basic monitoring program upon the release of "Ambient Air Quality Standards" in November 2011. The Pearl River Delta (PRD) region is the leading economic development region in South China, and thus its aerosol and ozone air pollution problems are also more apparent (Chan and Yao, 2008). Recent studies showed that fine particulate matter pollutions in the PRD region are aerosol-based, whereby $PM_{2.5}/PM_{10}$ and $PM_1/PM_{2.5}$ ratios can reach 0.65 and 0.86, respectively (Wu *et al.*, 2007, Deng *et al.*, 2008). Deng *et al.* (2013) pointed out there were relatively few studies on the composition of fine particulate matters that reduced visibility across the PRD region, and they proceeded by analyzing spectroscopy data in the Guangzhou area from July 2007 to March 2008. The analysis found that inorganic $PM_{2.5}$ in the PRD region were mainly comprised of sulfate, ammonium and nitrate aerosols, in which the proportions were 15%, 15% and 7%, respectively. Proportions of primary and secondary aerosols were both roughly 50%, but proportion of secondary aerosols increased with rising

* Corresponding author.
Tel.: +86-020-84112293; Fax: +86-020-84110692
E-mail address: eeswxm@mail.sysu.edu.cn

humidity. In cases with dry, 60% and 90% relative humidity, proportions of secondary aerosols were 59%, 75% and 84%, respectively, while proportions of sulfate aerosols were 15.8%, 22.5% and 28.2%, respectively.

Sulfate aerosols have strong extinction effect and are one of the major factors causing low atmospheric visibility. In addition, sulfates directly and indirectly affect radiation balance of the entire system and thus play an important role in regional and global climate changes (Charlson *et al.*, 1992; Chuang *et al.*, 1997; Ramanathan *et al.*, 2005). Photochemical reactions caused significant diurnal variation to sulfate aerosols, and atmospheric sulfur dioxide can react and be converted into sulfate through various liquid and gas-phase oxidation processes, in which liquid-phase oxidations are important to sulfate formation within clouds (Middleton *et al.*, 1980; Saxena and Seigneur, 1986; Seigneur and Saxena, 1988). The PRD region is located in Asia monsoon climate zone, during transition seasons between winter and summer monsoons, different weather conditions (including temperature, humidity and wind) will have various effects on homogeneous and heterogeneous chemical reaction processes, resulting in different aerosol compositions. Therefore, it is necessary to engage in corresponding research on the sources of sulfate aerosols, a major inorganic component of fine particulate matters, in the PRD region at specific weather conditions.

The process of forming sulfate aerosols through oxidations is mainly subject to the amount of SO_2 emitted from primary sources, amount of various oxidants and meteorological fields. Major oxidizing agents are hydroxyl radical (OH), hydrogen peroxide (H_2O_2), ozone (O_3), methylhydroperoxide (MHP) and peroxyacetic acid (PAA) (Seinfeld and Pandis, 1998). The sulfate tracking model within the Community Multi-scale Air Quality (CMAQ) model (Byun and Ching, 1999) is an effective tool in providing quantitative diagnosis on sulfate sources. Mathur *et al.* (2008) used CMAQ and sulfate tracking model to perform a simulation analysis on the generation and dissipation of sulfates over Eastern United States during summer 2004. The analysis compared simulation results with aircraft observation data in details, and showed that liquid-phase oxidation of H_2O_2 within clouds was the primary process in sulfate generation. Stein and Saylor (2012) also used sulfate tracking method to analyze sulfate oxidation pathways in the Eastern U.S., and found each of the three CMAQ chemical mechanism parameters (CBIV, CB05 and SAPRC99) could effectively simulate the changes in sulfate. All three parameters showed the two most significant oxidation pathways were by liquid-phase oxidation with H_2O_2 and gas-phase oxidation with OH radicals, but the third most significant oxidation pathway was different among parameters, in which CBIV suggested liquid-phase oxidation with MHP while CB05 and SAPRC99 yielded liquid-phase oxidation with PAA as results. Luo *et al.* (2011) used CMAQ to conduct a simulation analysis on the distribution of SO_2 and sulfate in the U.S. during summer 2002, and the results showed that sulfates were generated much more by aqueous reactions than by gaseous reactions, in which the proportion of sulfates generated by aqueous reactions can reach as high as 60%. On the other hand, there were almost no studies on sulfate generation for the PRD region using CMAQ and sulfate tracking model.

Before this study, the performance of WRF/SMOKE/CMAQ model and the characteristics of aerosol pollution in the PRD region during March 2012 have been analyzed and process analysis method were used to quantitatively compute the contribution of major physical and chemical processes to regional aerosol formation. Based on the understanding of the features of this aerosol pollution over the PRD region, the diagnostic analysis of sulfate aerosols formation by various oxidation processes over the PRD region was done. The main purposes of this paper were providing a quantitative diagnostic on the sources of sulfate using sulfate tracking, and investigating the impacts of humidity on sulfate generation process. Section 2 of this paper is an introduction of research methods, Section 3 is an analysis on observational data, Section 4 is an analysis on sulfate tracking results and Section 5 is the conclusion.

DATA AND METHODS

The WRF/SMOKE/CMAQ model system was performed using the triple-nested grid (Fig. 1(a)) centered at 23°N, 113°E with a 36/12/4 km horizontal resolution and 24 vertical layers. In Fig. 1(a), the black frames denote WRF grid domains and the red frames denote CMAQ grid domains. It is found that PRD region is surrounded by mountains and ocean with complex topography. Simulation time period ran from February 25 to March 28 2012. In the CMAQ model, each of the days was run separately. The initial and boundary conditions of CMAQ Chemistry-Transport Model (CCTM) simulation were generated from the previous CCTM simulation, except for the first-day run, in which they were generated from tabulated tropospheric vertical profiles. The Sparse Matrix Operator Kernel Emissions (SMOKE) model was used to process point, area and mobile emission sources for air quality model. The biogenic emissions were generated from the Model of Emissions of Gases and Aerosols from Nature (MEGAN). The merge step then combines the point, area, mobile and biogenic results to create model-ready emissions. The spatial distribution of $PM_{2.5}$ emissions presented in Fig. 1(b) shows high emissions in PRD region, especially in Guangzhou, Foshan and Shenzhen cities.

This paper used sulfate tracking method equipped in the CMAQ model for diagnosis of major sulfate aerosol sources. Sulfate tracking method can quantitatively calculate detailed information on various sulfate sources during CMAQ calculation, and it does not need any extra input data. Atmospheric sulfate aerosols are mainly formed from reactions between atmospheric sulfur dioxide and oxidants, and oxidants include hydroxyl radicals, ozone and etc. These reactions can be divided into gas-phase and liquid-phase reactions, in which liquid-phase reactions have greater contribution to sulfate generation. The process of sulfur dioxide reacting and converting into sulfate aerosols is controlled by many factors, such as concentration of oxidants, pH of cloud, dry and wet deposition rate of sulfur dioxide, and various meteorological fields (temperature, relative humidity, wind speed and etc.).

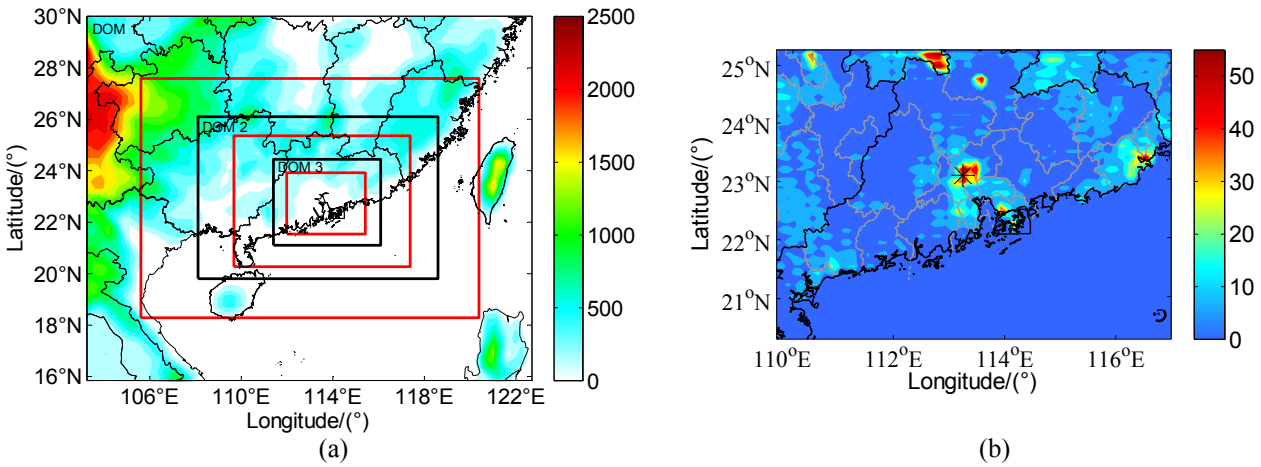

Fig. 1. (a) Terrain heights (Unit: m) in triple-nested modeling domains for WRF (black frames) and CMAQ (red frames) models. (b) Spatial distribution of hourly $PM_{2.5}$ emissions (Unit: g/s) in the second grid domain for CMAQ calculated by SMOKE. Black dot denotes the location of GYQ Monitoring Station (113.26°E, 23.16°N).

For gaseous chemical reactions, sulfate are mainly formed from oxidations between tetra sulfur S(IV) and hydroxyl radicals (OH):

$$S(IV) + OH \rightarrow S(VI) \quad (1)$$

For aqueous chemical reactions, sulfates are mainly formed by the five following reactions:

$$S(IV) + O_2(Mn^{2+}, Fe^{3+}) \rightarrow S(VI) \quad (2)$$

$$S(IV) + O_3 \rightarrow S(VI) \quad (3)$$

$$S(IV) + H_2O_2 \rightarrow S(VI) \quad (4)$$

$$S(IV) + MHP(CH_3OOH) \rightarrow S(VI) \quad (5)$$

$$S(IV) + PAA(C_3H_4O_2) \rightarrow S(VI) \quad (6)$$

whereas H_2O_2 denotes hydrogen peroxide, MHP denotes methylhydroperoxide and PAA denotes peroxyacetic acid.

Based on aforementioned gaseous and aqueous chemical reaction processes, sulfate tracking method quantitatively calculates the contribution of each reaction to sulfate level. There are several additional variables in CCTM output results when using sulfate tracking in CMAQ, namely ASO4AQH2O2J, ASO4AQO3J, ASO4AQFEMNJ, ASO4AQMHPJ, ASO4AQPAAJ, ASO4GAS, ASO4EMIS and ASO4ICBC, whereas they denote sources produced by oxidation reactions with hydrogen peroxide, with ozone, catalytic reactions with iron and manganese, oxidation reactions with MHP, with PAA, gas-phase chemical reactions, by direct emissions and by initial boundary conditions. Variable names containing AQ denote sources produced by liquid-phase chemical reactions and are corresponding to aforementioned chemical equations. For each variable, horizontal transport, diffusion and deposition are calculated independently, and source contribution on sulfate level at each grid point is given by last iteration. Sulfate tracking method is an effective tool to analyze the nonlinear generation sources of sulfate.

OBSERVATIONS ANALYSIS

Fig. 2 shows the temporal variations of temperature, relative humidity, wind speed and direction measured at Gongyuanqian (GYQ) Monitoring Station (23.16°N, 113.26°E, located in Guangzhou city, shown in Fig. 1(b)). There were three pollution episodes as seen from Fig. 3(a), namely March 1–5, 13–21 and 25–27, respectively. The temperature series showed that there were three warming periods and two cooling periods in the PRD region during March 2012, in which the three pollutant episodes occurred during these three warming periods, respectively. Besides, lower wind speed went against the diffusion of local emitted pollutants and caused these pollution episodes. During the first two pollution episodes, the PRD region was under the influence of southeasterly warm and wet air flow with relative humidity maintained at a high level, which was favorable to the secondary transformation of precursors. During the third pollution episode, the PRD region was in the influenced by northeasterly dry air flow with lower relative humidity.

Fig. 3 showed the time series of $PM_{2.5}$, PM_{10}, visibility, sulfate (SO_4^{2-}) and nitrate (NO_3^-) concentrations recorded at GYQ Monitoring Station in March 2012. The $PM_{2.5}$ and PM_{10} concentrations were measured by a tapered element oscillating microbalance (TEOM RP1400a) ambient particulate monitor. PM_{10} concentration increased during the three pollution processes, with peak values of 216 μg/m^3, 191 μg/m^3 and 165 μg/m^3, respectively. $PM_{2.5}$ concentration was higher during the first two pollution episodes and reached a maximum of 195 μg/m^3 (March 4) and 114 μg/m^3 (March 17), respectively. Particulate matters, especially fine particles, have an extinction effect on visibility. Due to higher $PM_{2.5}$ and PM_{10} concentrations, visibility was lower during the first two episodes and had a minimum of 2.3 km and 2.6 km, respectively. However, $PM_{2.5}$ concentration was

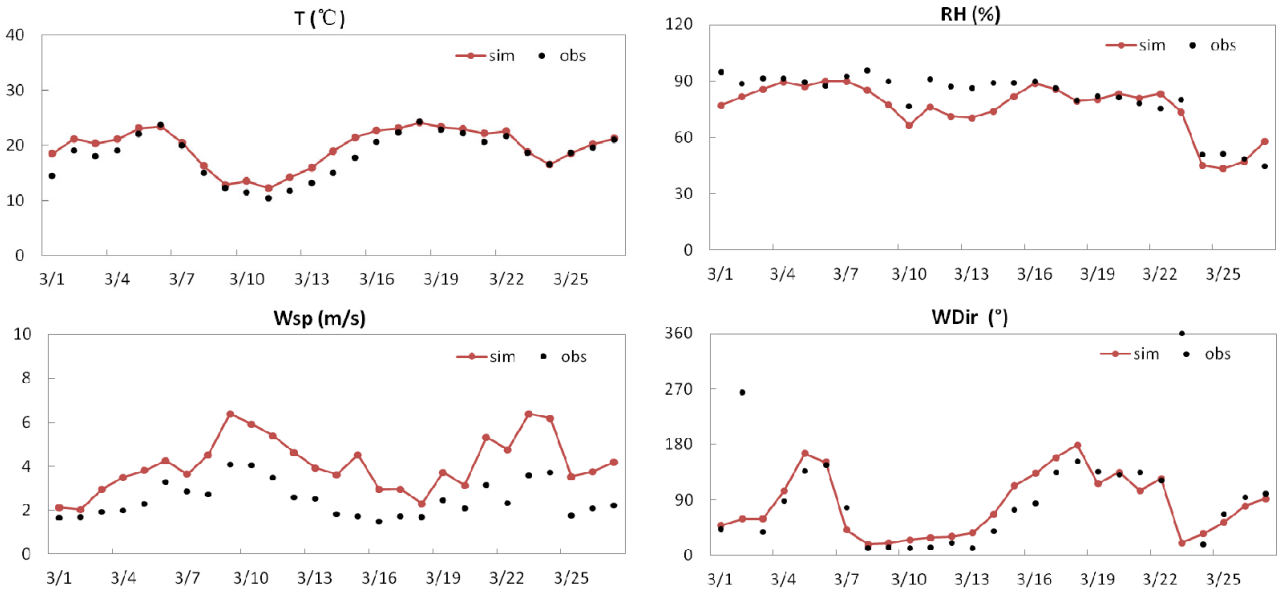

Fig. 2. Simulated and measured meteorological elements at GYQ Monitoring Station during March 2012.

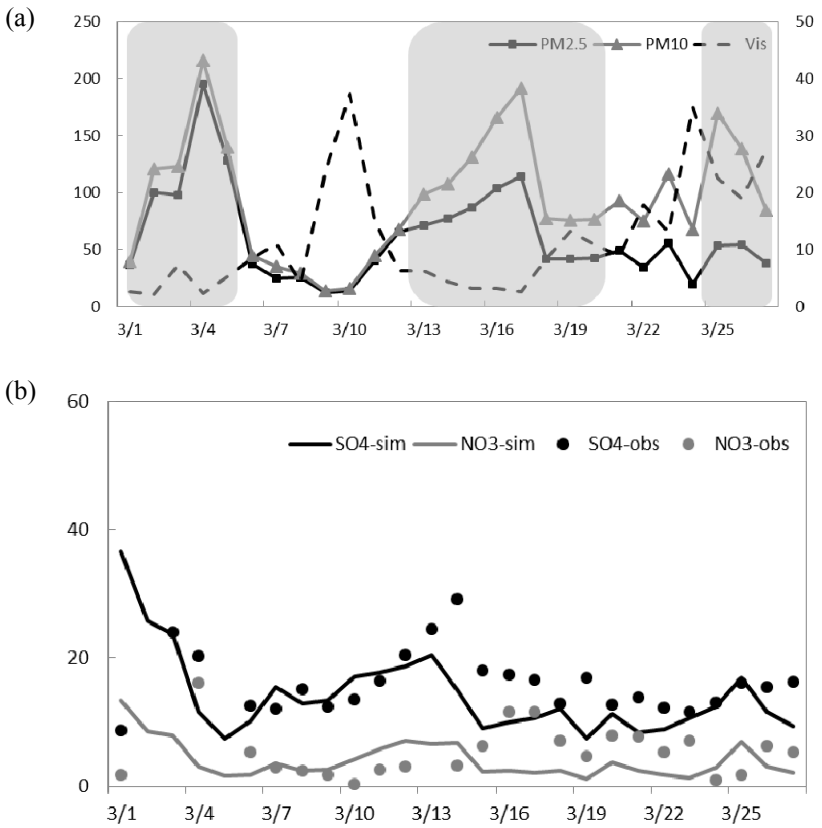

Fig. 3. (a) Time series of $PM_{2.5}$ concentration, PM_{10} concentration and visibility recorded at GYQ Monitoring Station in March 2012. The shaded vertical areas denote three pollution episodes. (b) Time series of simulated and measured daily averaged sulfate and nitrate concentrations.

lower but PM_{10} concentration was higher during the third episode. For SO_4^{2-} and NO_3^- concentrations, sulfate contributed far more to $PM_{2.5}$ than nitrate during all three pollution episodes, in which sulfate accounted for 30% of $PM_{2.5}$ at maximum while nitrate accounted for only 10% at maximum. Prior to March 17, sulfate and nitrate had higher concentrations due to ample water vapors in the atmosphere, except for a brief period between March 6–11, whereas

precipitation served as clearing effect. Then, after March 17, sulfate and nitrate concentrations trended lower as relative humidity slightly decreased. Finally, after March 23, nitrate concentration dropped rapidly as humidity and temperature further declined, but it recovered as temperature rose afterward; however, sulfate concentrations did not change significantly during this period.

Sulfates and nitrates are major inorganic components of atmospheric secondary aerosols, and are converted from atmospheric sulfur dioxide and nitrogen oxides through a series of chemical reactions. Mass concentration of secondary aerosols depends on the concentration of their precursors, atmospheric gas-particle conversion rate and local weather conditions, principally temperature and relative humidity. To investigate secondary conversion of gaseous pollutants, we used Sulfur Oxidation Ratio (SOR) and Nitrogen Oxidation Ratio (NOR) to measure the degree of secondary conversion. Greater SOR and NOR values indicate that there are more gas converted into secondary aerosols. Values greater than 0.1 suggest there are photochemical oxidations occurred in the atmosphere; values less than 0.1 mean atmospheric pollutants mostly consisted of primary pollutants. The equation for SOR and NOR are as follows:

$$\mathrm{SOR} = \frac{[\text{nss-}SO_4^{2-}]/96}{[\text{nss-}SO_4^{2-}]/96 + [SO_2]/64} \quad (7)$$

$$\mathrm{NOR} = \frac{[NO_3^-]/62}{[NO_3^-]/62 + [NO_2]/46} \quad (8)$$

whereas nss-SO_4^{2-} denotes non-sea-salt sulfate. Given $SO_4^{2-}/Na^+ = 0.251$ for sea salt particles and assumed Na^+ within aerosols are primarily came from sea salt, the value for sea salt sulfate, nss-SO_4^{2-}, is derived from SO_4^{2-}/Na^+ ratio. The nss-SO_4^{2-} is calculated as follows:

$$[\text{nss-}SO_4^{2-}] = [SO_4^{2-}] - 0.251 \times [Na^+] \quad (9)$$

Fig. 4 showed the calculated SOR and NOR values at GYQ Monitoring Station in March 2012. SOR was much greater than 0.1 and between 0.18–0.66 throughout March, which indicating there was substantial atmospheric SO_2 converted into secondary sulfate aerosols through gaseous or aqueous oxidation. Meanwhile, NOR was below 0.1 in the whole of March except on the 4th when it reached 0.2, and this indicated there were only small amounts of atmospheric NO_x converted into NO_3^-. During the first two pollution episodes, relative humidity was higher than that during the third episode, and studies have shown that high humidity conditions are favorable for converting SO_2 and NO_x into sulfates and nitrates, resulting in larger $PM_{2.5}/PM_{10}$ ratio. In addition, wind speed was slow during these two episodes, atmospheric diffusion was weak and thereby secondary aerosols accumulated near the ground, resulting in high particulate matter concentration and serious pollution. In contrast, during the third pollution episode, SOR was not high relatively and NOR was small due to low humidity during this period. The humidity condition was not favorable for SO_2 liquid-phase conversion and additionally a very low wind speed during this episode resulting in higher PM_{10} concentration. As a result, $PM_{2.5}/PM_{10}$ ratio was not high and was between 31–45%.

RESULTS ANALYSIS

WRF/SMOKE/CMAQ model system was utilized to simulate the aerosol pollution processes during March 2012 in the PRD region. The model system used a triple-nested grid with a 36/12/4 km horizontal resolution and 24 vertical layers (the altitudes of the lower 15 layers are 25 m, 65 m, 120 m, 200 m, 280 m, 400 m, 560 m, 730 m, 900 m, 1065 m, 1240 m, 1415 m, 1590 m, 1820 m and 2100 m, respectively). Simulation time period ran from February 25 to March 28 2012. In all, the model system performed fairly well in simulating meteorological and chemical fields. Fig. 2 shows the comparison between model simulation and March 2012 measured data from GYQ Monitoring Station. It was found that WRF model was capable of capturing the variations of each meteorological element, including three warming periods and two passages of cold front in the whole month, but wind speed returned from model simulation had a positive bias. The correlation coefficient of simulated temperature, relative humidity, and wind speed with the observations were 0.94, 0.84 and 0.77, respectively. CMAQ model had a better performance in simulating $PM_{2.5}$, SO_2 and NO_x concentration and was able to reproduce variation patterns for the concentration of each pollutant. Index of

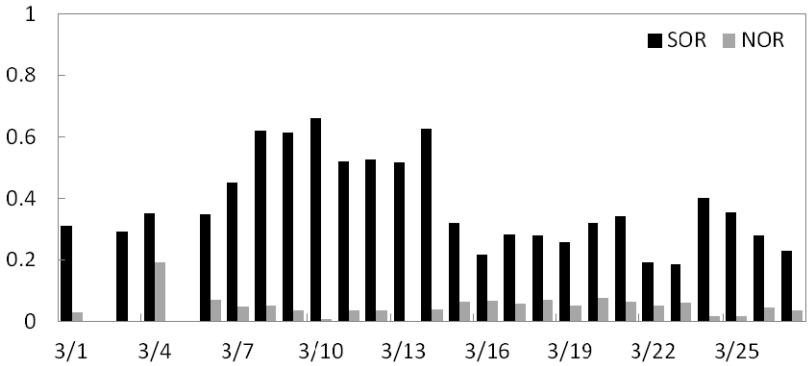

Fig. 4. Time series of SOR and NOR at GYQ Monitoring Station in March 2012.

agreement (IOA) is a statistical measure defined as:

$$\mathrm{IOA} = 1 - \frac{\sum_{i=1}^{n}(O_i - S_i)^2}{\sum_{i=1}^{n}\left(\left|O_i - \bar{O}\right| + \left|S_i - \bar{S}\right|\right)^2} \quad (10)$$

whereas S denotes the model simulations and O denotes the observations. Model performs better with IOA close to 1. The results showed that simulated values exhibited large degree of agreement with measured data as IOA were all above 0.8 for various air pollutants (PM_{10}, $PM_{2.5}$, SO_2, NO_x and O_3). Due to the uncertainty of upwind emissions in CMAQ simulation, simulated absolute PM_{10} values were lower than measured data throughout late March.

In addition, process analysis method was used to understand the contribution from various physical and chemical processes to particulate matter. The results showed that concentration of particulate matters was contributed by different processes in lower and upper layers. Emission source, vertical and horizontal transport were the primary contributors to pollutant concentration in lower layers, while vertical and horizontal transport, aerosol process and cloud process were the major contributors in upper layers. Cloud process had greater contribution when relative humidity was high, and had a positive contribution to particulate matter concentration.

Based on the aforementioned results, sulfate tracking method was utilized to diagnostic the formation mechanism of sulfate aerosol. Fig. 3(b) showed the daily average sulfate and nitrate concentrations from the CMAQ model simulations and measured data at GYQ Monitoring Station. As seen from the figure, CMAQ simulated concentrations were close to actual observed values with no order of magnitude differences, wherein measured and simulated daily average sulfate concentrations for March 2012 were 16.1 μg/m^3 and 12.7 μg/m^3, respectively, while measured and simulated daily average nitrate concentrations were 5.3 μg/m^3 and 3.6 μg/m^3. However, the model underestimated concentrations between March 15–21, with simulated sulfate and nitrate concentrations were 43% and 70% lower, respectively. From simulated $PM_{2.5}$ composition diagrams (Fig. 5) for each of the three pollution episodes at GYQ Monitoring Station in March 2012, sulfate, OC and PM_{other} were significant constituents of fine particulate matters, but the amount of nitrates was small. This was due to nitrate having higher volatility and is more difficult to exist in aerosol form, thereby requiring a certain level of humidity to allow nitrate to exist in aqueous form. Meanwhile, $PM_{2.5}$ composition is different for different pollution episode. Given that relative humidity was higher during the first two episodes, the atmosphere was favorable for liquid-phase oxidation reaction and a large number of secondary aerosols were formed, and additionally hydrophilic aerosols underwent hygroscopic growth under high humidity. As a result, proportion of sulfate, nitrate and ammonium significantly increased, and all three accounted for 50% and 56% of aerosols in the first two episodes, respectively. Meanwhile,

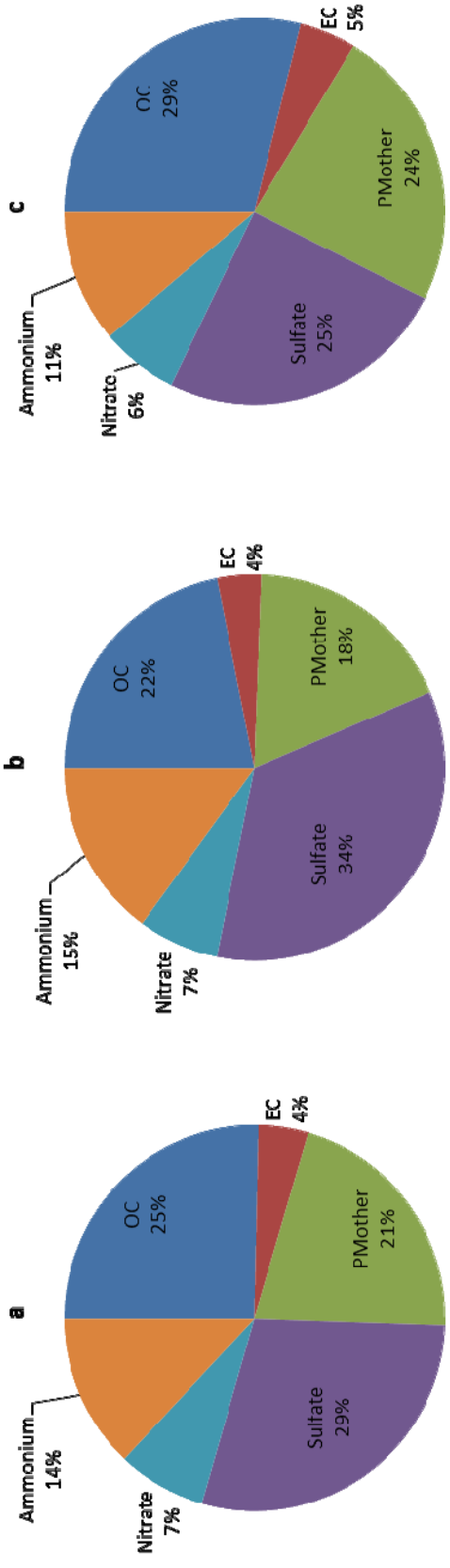

Fig. 5. Simulated aerosol composition at GYQ Monitoring Station for each pollution episodes (a: March 4; b: March 17; c: March 26).

there were fewer aqueous chemical reactions during the third pollution episode because of the lower relative humidity, and so the proportions of sulfate, nitrate and ammonium were lower and only accounted for only 42% of aerosols in total. In contrast, proportions of OC, EC and PM_{other} increased. Comparison with previous field experiments in the PRD region (Hagler, 2006) showed that simulated results had similar aerosol composition distribution with actual condition, and thereby suggested CMAQ model is effective to simulate aerosol composition.

Sulfates are important factor for extinction coefficient that affects visibility. Sulfate accounts for more than 25% of total $PM_{2.5}$ in the PRD region. Analysis on sulfate sources would help exploring the primary causes for formation of secondary aerosols in the PRD region.

Fig. 6(a) depicted simulated sulfate concentrations across various heights above GYQ Monitoring Station. The figure showed that high sulfate values occurred during March 1–5, 13–21 and 25–27, corresponding to each of the three pollution episodes respectively. Sulfate concentrations were higher during the first two episodes than the third one, and were due to distribution of the relative humidity field. Since humidity was lower during the third episode, there were less sulfur dioxide converted to sulfate and thus the sulfate concentration level was lowered. Vertical distribution showed that sulfate concentration decreased with height, whereby the maximum occurred at the near-surface layer. For the first two pollution episodes, the height in which sulfate concentration was greater than 10 μg/m^3 was up to the 7th layer of the model (560 m or so), while it was up to

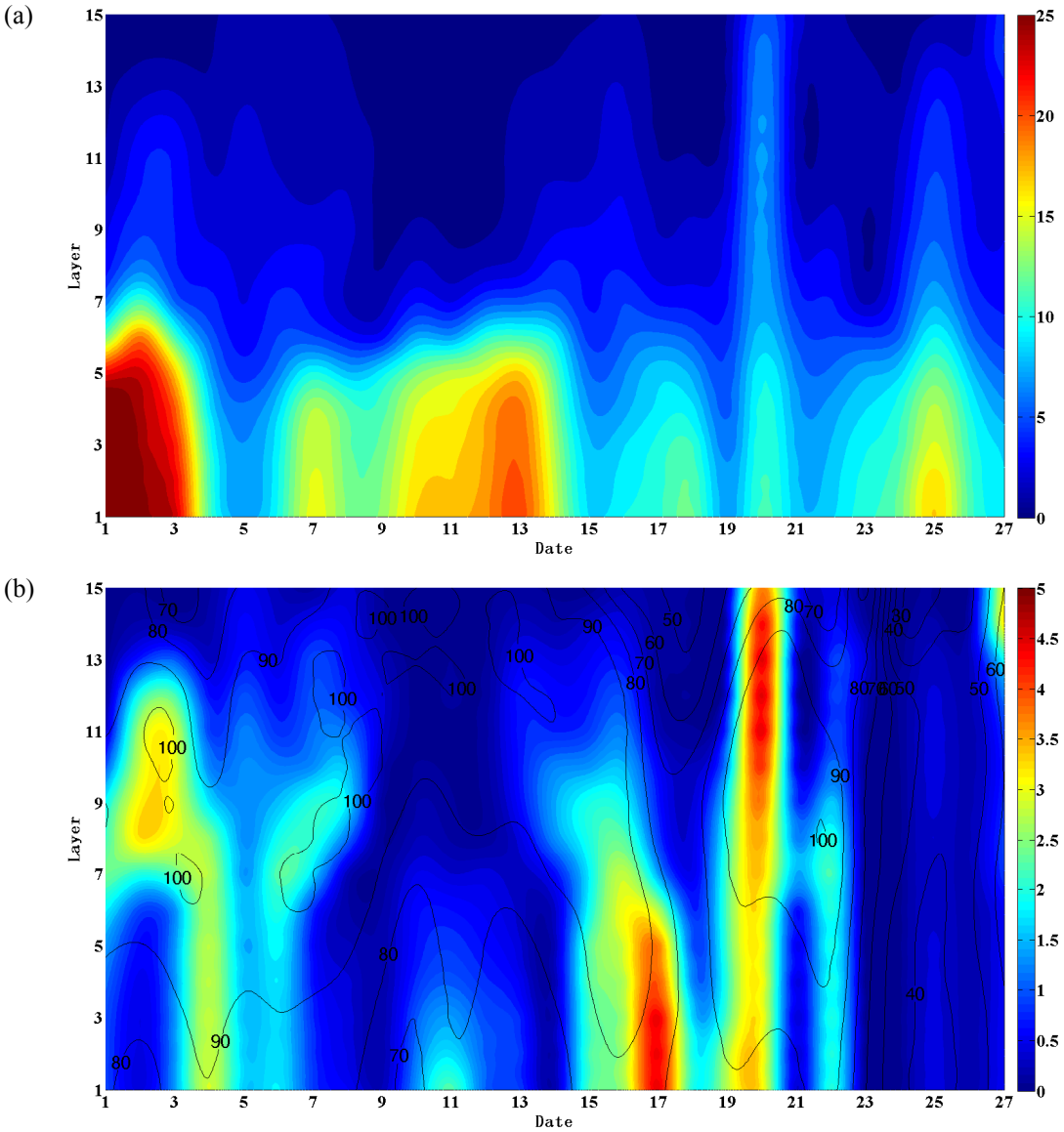

Fig. 6. (a) Simulated sulfate aerosol concentration (unit: μg/m^3) above GYQ Monitoring Station. (b) Simulated relative humidity (Contour line; Unit: %) and secondary sulfate aerosol concentration (Shaded; Unit: μg/m^3) above GYQ Monitoring Station. (The altitudes of 15 layers are 25 m, 65 m, 120 m, 200 m, 280 m, 400 m, 560 m, 730 m, 900 m, 1065 m, 1240 m, 1415 m, 1590 m, 1820 m and 2100 m, respectively).

the 5th layer (280 m or so) for the third episode. Sulfate concentrations were lower at all heights during the third episode than the first two.

Fig. 6(b) showed the cross-sectional time series of relative humidity and secondary sulfate aerosols above GYQ Monitoring Station. Relative humidity was high throughout the entire atmospheric boundary layer (altitude of the 15th layer of the model was around 2100m) during March 1–23 and was higher than 70%. Humidity was significantly lower during March 23–27 at only about 40%. As a result, high relative humidity conditions made more sulfur dioxides undergo aqueous chemical reactions and converted into sulfate, in which to some extent, explained why $PM_{2.5}$ accounted for higher proportion of PM_{10} during the first two pollution episodes. Furthermore, higher humidity during the first two episodes provided favorable conditions for hygroscopic growth of fine particulate matters, resulting in significantly lower visibility. The vertical distribution showed that relative humidity was higher at upper levels within atmospheric boundary layer than at near-surface layers. Unlike total sulfate, secondary sulfate concentrations at upper levels could be higher than that at ground level. The height at which relative humidity exceeded 90% was at layers 7–9 of the model during the first episode, while it was at layers 11–15 during the second episode, wherein there were more secondary sulfate aerosols generated by liquid-phase chemical reactions at these heights. During the third pollution episode, less secondary sulfate was generated due to lower relative humidity.

Fig. 7(a) showed the time series of source contribution of various processes to sulfate level at near-surface layer in GYQ Monitoring Station, in which ICBC denotes contribution of initial field and boundary conditions, EMIS denotes contribution of direct emissions, GAS denotes contribution of reactions between S(IV) and OH, PAA, O_3, MHP, H_2O_2 and FEMN denotes contribution of reactions between respective chemicals and S(IV) through liquid-phase oxidation or catalytic conversion. As seen from the figure, the largest contributions came from direct emissions and initial conditions. Among chemical reaction contributions, sulfates were mainly generated by catalytic conversion by H_2O_2 and FEMN and oxidation with O_3, while gas-phase oxidation, PAA and MHP reactions provided little contributions. From the time series of contributions, there were two periods with high values of contribution rate from liquid-phase chemical reactions, namely during March 4–6 and March 15–23, in which all liquid-phase reactions contributed about 20% of sulfate level in total. This is because relative humidity was high during these two periods, and temperature also rose due to the corresponding southerly warm and humid air flow system. Hence, higher temperature and relative humidity were favorable for sulfur dioxide to undergo liquid-phase oxidation and generate secondary sulfate aerosols. These two periods coincided with the first two

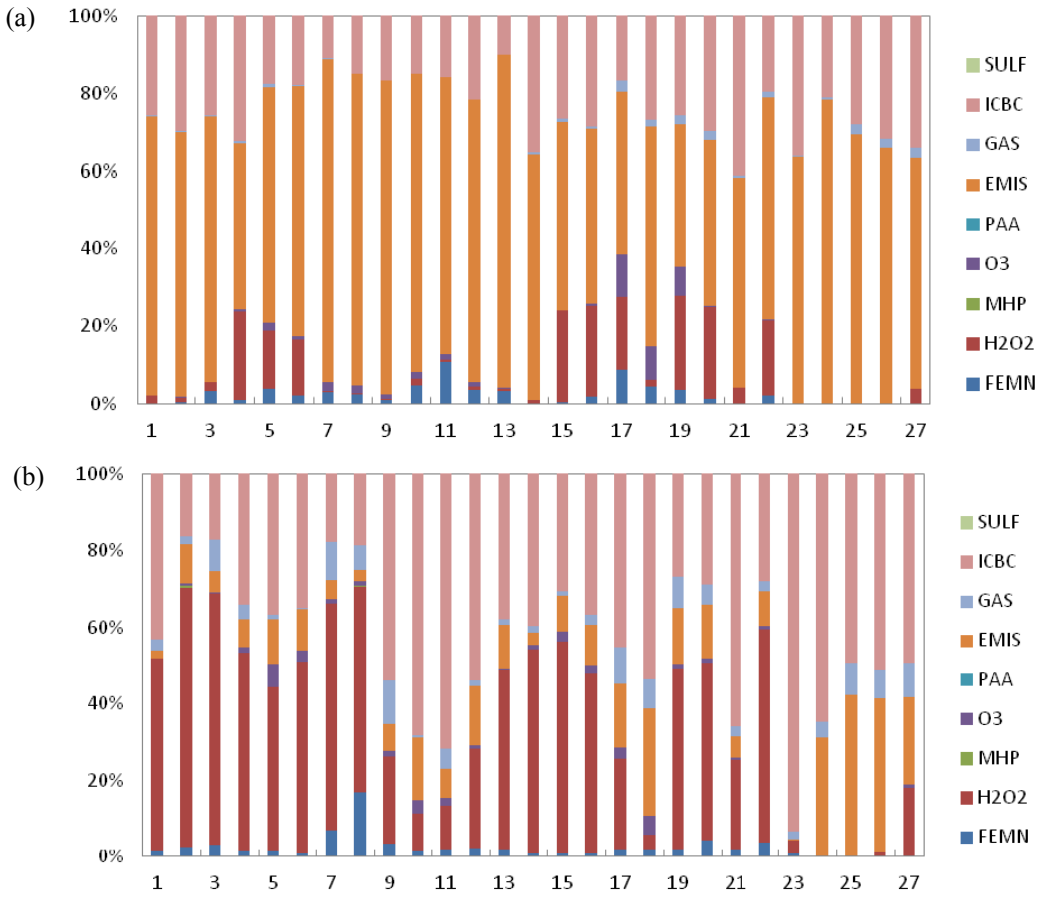

Fig. 7. Simulated contribution rates to sulfate level at 1st (a) and 9th (b) model layer at GYQ Monitoring Station.

pollution episodes, thereby indicating the first two episodes had a significant amount of secondary sulfate aerosols were generated by liquid-phase reactions. Meanwhile, there were almost no contributions from liquid-phase reactions during the third pollution episode, in which sulfates were generated by direct emissions, boundary and initial conditions, with a small contribution of gas-phase reactions.

Fig. 7(b) showed the time series of source contribution of each process to sulfate level at the 9th layer above GYQ Monitoring Station. As seen from the figure, direct emission contributed significantly less at upper layer than at near-surface layer, with its contribution reduced from around 60% to 10%. Given that relative humidity was higher at the upper layer and provided favorable conditions for liquid-phase reactions of S(IV), contribution of liquid-phase catalytic oxidation to sulfate generation was significantly increased, in which the contribution rate was greater than 40% between March 1–23, particularly during the first two pollution episodes when contribution of liquid-phase oxidation reached 50%. Among liquid-phase oxidation reactions, reaction between S(IV) and H_2O_2 was the primary reaction when other types had lower contributions. Furthermore, the second-most significant contributor to sulfate level was boundary and initial conditions, in which this contribution rate had increased when compared with lower layers, mainly since the contribution of direct emissions had dropped significantly as altitude increased, leading to contribution of boundary and initial conditions gradually became prominent.

Fig. 8 showed the vertical distribution of source contribution to sulfate level during each of the three pollution process, in which black dots denote relative humidity at the corresponding layer. As seen from the figure, contribution of direct emissions decreased with increasing height for all three episodes. By contrast, contribution of boundary and initial conditions increased with increasing height and accounted for more than 80% of sulfate sources at the 15th layer of the model. Besides direct emissions and boundary and initial conditions, liquid-phase oxidation reaction between S(IV) and H_2O_2 was the most significant contributor during the first two pollution episodes, and it was closely correlated with relative humidity. On March 4, the Guangzhou area was under the influence of southerly warm and humid air flow system, relative humidity was high and exceeded 80% throughout the atmospheric boundary layer, of which the highest readings occurred within the 7th to 13th layer of the model. The corresponding contribution rate of liquid-phase oxidation reaction between S(IV) and H_2O_2 was also at the highest within these layers and exceeded 40%. Then, on March 17, the Guangzhou area was also under the influence of southerly warm and humid air flow system, but relative humidity was lower than during the first pollution episode, in which humidity was above 80% only for lower layers within the boundary layer and hovered around 60% for layers above the 8th layer of the model. Consequently, contribution of liquid-phase oxidation reaction between S(IV) and H_2O_2 remained at around 20% for the second pollution episode. Compared with the first episode, besides liquid-phase oxidation between S(IV) and H_2O_2, there was considerable contribution of liquid-phase oxidation reaction between S(IV) and O_3 during the second pollution episode, and it contributed around 10% in the near-surface layer. In addition, contribution of catalytic oxidation with Fe and Mn also reached 8% in the near-surface layer. During the first two pollution episodes, relative humidity was high and thus atmospheric liquid-phase reactions were very active and generated large amount of sulfate; highest rate for contribution of liquid-phase oxidation occurred in layers with highest relative humidity. Meanwhile, relative humidity was lower at 40% during the third pollution episode, so direct emissions and boundary and initial conditions were the major contributors to sulfate level for this episode, and gas-phase oxidation reaction also accounted for about 3% of contribution. In conclusion, the first two pollution episodes contained more fine particulate matters generated by secondary reactions, and thus, $PM_{2.5}/PM_{10}$ was higher resulting in lower visibility. In contrast, there were little sulfate generated by liquid-phase reactions during the third episode, in which fine particulate matter concentration was low and pollutants were primarily coarse particles, and thus $PM_{2.5}/PM_{10}$ was lower resulting in higher visibility.

Figs. 9(a) and 9(b) showed the time series of contribution of each process to sulfate level at ground level on March 15 and March 26, respectively, whereas black dots represent relative humidity. As seen from the figure, contribution of initial and boundary conditions was set as 100% in the first hour of the day, and it gradually decreased over time. Contribution of emissions rose rapidly during the first two hours and remained stable at above 50% starting from the third hour. Given relative humidity was higher during the first pollution episode, contribution of liquid-phase reactions was also greater, and as humidity began to steadily increase at 07:00 (Universal Time), contribution of hydrogen peroxide also began to increase and rose to more than 40% at 10:00. This contribution rate from hydrogen peroxide exceeded that from emissions and reached 52% and 51% at 19:00 and 21:00, respectively, when relative humidity were close to 100% at these time. Other types of liquid-phase oxidation processes had smaller contribution to sulfate level. Due to relatively lower humidity during the third pollution episode, in which relative humidity was essentially less than 60% on March 26, contribution of liquid-phase reaction was very small and sulfates were mainly generated by emissions, initial and boundary condition inputs and gas-phase oxidation processes. Contribution of gas-phase oxidation mainly occurred during March 7–14, with the highest contribution rate of 13.3%.

Sulfates at upper layers were less affected by emissions (Figs. 9(c) and 9(d)), and contribution of initial and boundary conditions decreased rapidly during the first few hours of the day. On March 15, contribution of liquid-phase oxidation was significantly greater than at ground level due to relative humidity was very high (close to saturation). Contribution of reaction between S(IV) and hydrogen peroxide, in particular, its rate rose above 60% at 07:00 and reached the maximum of 76.3% at 23:00. In contrast, contributions from other liquid-phase oxidation were smaller. On the other hand, relative humidity was lower before 19:00 on March 26, contribution of liquid-phase oxidation reaction was very

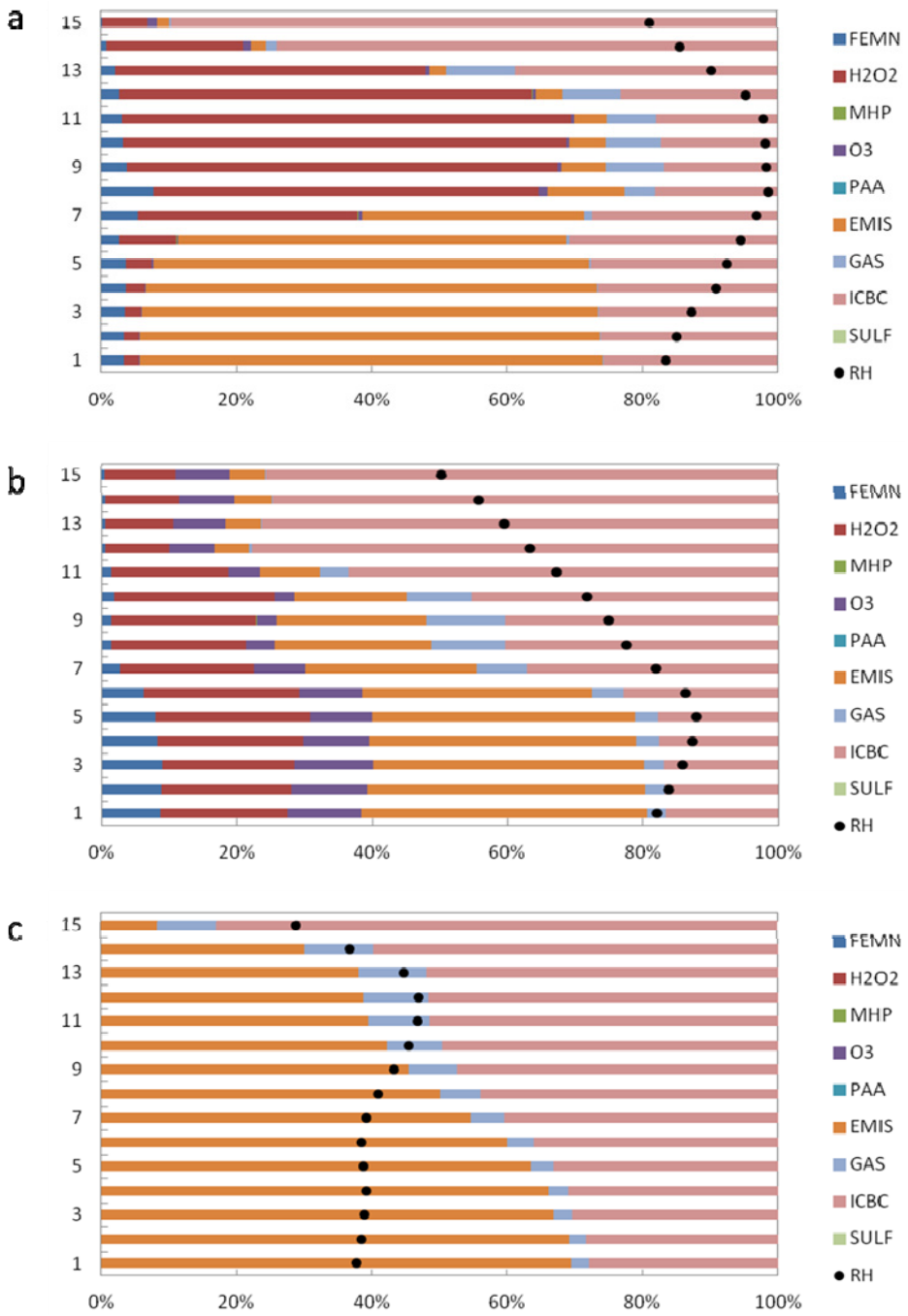

Fig. 8. Vertical distribution of contribution rates to sulfate level from each process (a: March 4; b: March 17; c: March 26).

small, and sulfates at upper layers were more prominently affected by initial conditions and emissions. However, as relative humidity began to increase after 19:00, contribution rate from liquid-phase chemical reactions also increased and reached 10%. Therefore, sulfates at upper layers during the third pollution episode were mainly contributed from initial and boundary condition inputs, direct emission and gas-phase oxidation reactions.

CONCLUSION

This paper used sulfate tracking method to analyze the sources of sulfates among secondary aerosols over the PRD region during March 2012. The results showed that:

(1) Three pollution episodes occurred during March 2012, in which the first two episodes were caused mostly by fine particulate matters while the third one mainly caused by coarse particulate matters. Given that fine particulate matters have stronger extinction effect, visibility was lower during the first two pollution episodes and reached as low as 2 km. Sulfate oxidation rate was between 0.18–0.66 throughout March, which meant there were large number of atmospheric SO_2 reacted and was converted into secondary sulfate aerosols through liquid or gas-phase

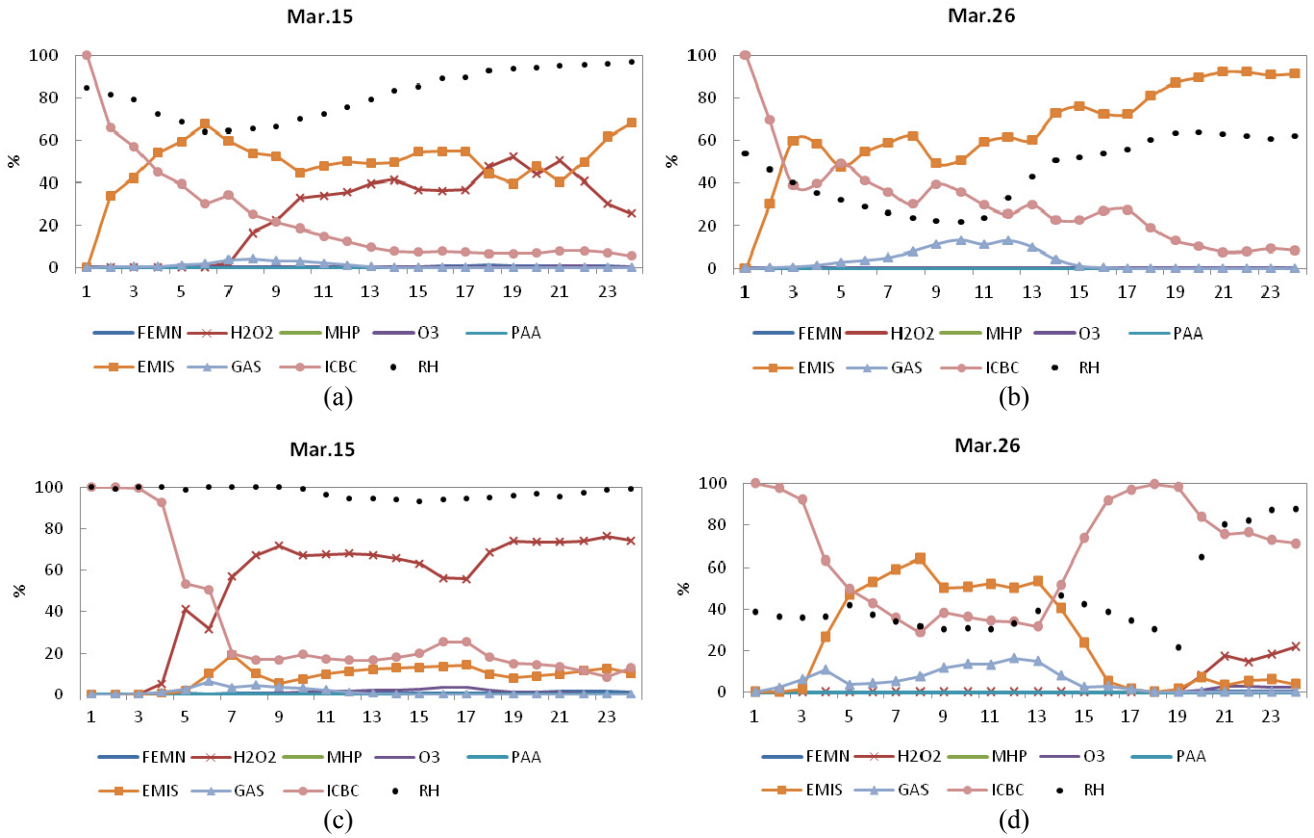

Fig. 9. Contribution rates to sulfate level from each process and relative humidity at ground level on March 15 (a) and March 26 (b). (c) and (d) are the same as (a) and (b), but at 9th model layer (altitude: 900 m).

oxidation reactions. On the other hand, nitrate oxidation rate was below 0.1 except for reaching 0.2 on March 4, which indicated there were less amounts of atmospheric NO_x converted into NO_3^-, and sulfate aerosols were the main inorganic component of fine particulate matters.

(2) For all three pollution episodes, besides direct emissions, boundary and initial conditions, the major sources of sulfate was from liquid-phase oxidations and gas-phase oxidations, in which contribution of liquid-phase oxidation was closely related with relative humidity. The first two pollution episodes occurred under the influence of southerly warm and humid air flow system, southerly winds brought high humidity and provided favorable conditions for active liquid-phase oxidation reactions, thus forming larger volume of sulfate in the atmosphere. Contribution of liquid-phase oxidation mainly consisted of liquid-phase oxidation with of H_2O_2, catalytic oxidation with Fe and Mn, and liquid-phase oxidation with O_3, while liquid-phase oxidation with PAA and MHP provided very little contribution. Meanwhile, relative humidity was lower during the third pollution episode, so contribution of liquid-phase oxidation was small and contribution of gas-phase oxidation between S(IV) and OH was larger.

(3) The concentration of sulfate aerosols decreased with increasing height, with the value of 10 μg/m^3 in the 5th–7th layer of the model (about 280–560 m in altitude). In the order of significance, the four main contributors to near-surface sulfates were direct emissions, boundary and initial conditions, liquid-phase oxidations with H_2O_2, and catalytic oxidation reaction with Fe and Mn. At upper layers, direct emissions had fewer impacts on sulfate level, whereas contribution of liquid-phase catalytic oxidation increased significantly and liquid-phase oxidations were mainly consisted of reactions between S(IV) and H_2O_2. The four main contributors to sulfate level at upper layers were, in the order of significance, liquid-phase oxidation with H_2O_2, boundary and initial conditions, direct emissions and gas-phase oxidation.

(4) The comparison between the hourly contribution rates on ground-level sulfates for the two pollution episodes occurred on March 15 and March 26 found that: the sum between contribution of direct emissions and initial and boundary conditions was close to 100% within the first few hours of the day; contribution of hydrogen peroxide oxidation increased with rising relative humidity, and the rate may exceed the contribution rate of direct source if relative humidity was close to 100%; contribution of gas-phase oxidations between S(IV) and OH was greater when relative humidity was lower; for high-altitude sulfates, contribution rate of reactions between S(IV) and hydrogen peroxide can exceeded 60% when relative humidity is high, and became the greatest contributor on sulfate level.

ACKNOWLEDGEMENTS

This research was supported by funds from National Natural Science Foundation 41275100, 41275018, public

sector (meteorological) scientific research project (GYHY201306042, GYHY201406031), EU project PANDA and National Natural Science Foundation of Guangdong Province as key project (S2012020011044). Thanks Guangzhou Environmental Monitoring Station for providing the air quality data. Thanks for the support of High level Talents project of GuangDong province. The Network and Information Technology Center at Sun Yat-sen University is acknowledged for providing the use of computers in the research.

REFERENCES

Byun, D.W. and Ching, J.K.S. (1999). Science algorithms of the EPA Models-3 Community Multi-scale Air Quality (CMAQ) Modeling System, Washington, D. C.: U.S. Environ. Prot. Agency, U.S. Govt. Print. Office.

Chan, C.K. and Yao, X.H. (2008). Air Pollution in Mega Cities in China. *Atmos. Environ.* 42: 1–42.

Charlson, R.J., Schwartz, S.E., Hales, J.M., Cess, R.D., Coakley, J.A. Jr., Hansen, J.E. and Hofmann, D.J. (1992). Climate Forcing by Anthropogenic Aerosols. *Science* 255: 423–430.

Chuang, C.C., Penner, J.E., Taylor, K.E., Grossman, A.S. and Walton J.J. (1997). An Assessment of the Radiative Effects of Anthropogenic Sulfate. *J. Geophys. Res.* 102: 3761–3778.

Deng, X.J., Tie, X.X., Wu, D., Zhou, X.J., Bi, X.Y., Tan, H.B., Li, F. and Jiang, C.L. (2008). Long-term Trend of Visibility and Its Characterizations in the Pearl River Delta Region (PRD), China. *Atmos. Environ.* 42: 1424–1435.

Deng, X.J., Wu, D., Yu, J.Z., Lau, A.K.H., Li, F., Tan, H.B., Yuan, Z.B., Ng, W.M., Deng, T., Wu, C. and Zhou, X.J. (2013). Characterization of Secondary Aerosol and Its Extinction Effects on Visibility over the Pearl River Delta Region, China. *J. Air Waste Manage. Assoc.* 63: 1012–1021.

Hagler, G.S.W., Bergin, M.H., Salmon, L.G., Yu, J.Z., Wan, E.C.H., Zheng, M., Zeng, L.M., Kiang, C.S., Zhang, Y.H., Lau, A.K.H. and Schauer, J.J. (2006). Source Areas and Chemical Composition of Fine Particulate Matter in the Pearl River Delta Region of China. *Atmos. Environ.* 40: 3802–3815.

Luo, C., Wang, Y.H., Mueller, S. and Knipping, E. (2011). Diagnosis of an Underestimation of Summertime Sulfate Using the Community Multiscale Air Quality Model. *Atmos. Environ.* 45: 5119–5130.

Mathur, R., Roselle, S., Pouliot, G. and Sarwar, G. (2008). Diagnostic Analysis of the Three-Dimensional Sulfur Distributions over the Eastern United States Using the CMAQ Model and Measurements from the ICARTT Field Experiment, In *Air Pollution Modeling and Its Application XIX,* Borrego, C. and Miranda, A.I. (Eds.), p. 496–504.

Middleton, P., Kiang, C.S. and Mohnen, V.A. (1980), Theoretical Estimates of the Relative Importance of Various Urban Sulfate Aerosol Production Mechanisms. *Atmos. Environ.* 14: 463–472.

Ramanathan, V., Chung, C., Kim, D., Bettge, T., Buja, L., Kiehl, J.T., Washington, W.M. and Fu, Q. (2005). Atmospheric Brown Clouds: Impacts on South Asian Climate and Hydrological Cycle. *Proc. Nat. Acad. Sci. U.S.A.* 102: 5326–5333.

Saxena, P. and Seigneur, C. (1986). The Extent of Nonlinearity in the Atmospheric Chemistry of Sulfate Formation. *J. Air Pollut. Contr. Assoc.* 36: 1151–1154.

Seigneur, C. and Saxena, P. (1998). A theoretical Investigation of Sulfate Formation in Clouds. *Atmos. Environ.* 22: 101–115.

Seinfeld, J.H. and Pandis, S.N. (1998). *Atmospheric Chemistry and Physics: From Air Pollution to Climate Change*, John Wiley & Sons, Inc., New York.

Stein, A.F. and Saylor, R.D. (2012). Sensitivities of Sulfate Aerosol Formation and Oxidation Pathways on the Chemical Mechanism Employed in Simulations. *Atmos. Chem. Phys. Discuss.* 12: 8169–8182, doi: 10.5194/acpd-12-8169-2012.

Wu, D., Bi, X., Deng, X. J., Li, F., Tan, H., Liao, G. and Huang, J. (2007). Effect of Atmospheric Haze on the Deterioration of Visibility over the Pearl River Delta. *Acta Meteorol. Sin.* 21: 215.

Received for review, March 2, 2014
Revised, May 20, 2014
Accepted, June 10, 2014